*Korean J. Chem. Eng.*, 33(12), 3388-3400 (2016)
DOI: 10.1007/s11814-016-0232-1

pISSN: 0256-1115
eISSN: 1975-7220

# Rapid transesterification of *Jatropha curcas* oil to biodiesel using novel catalyst with a microwave heating system

**Achanai Buasri*,**,†, Methasit Lukkanasiri*, Raviporn Nernrimnong*, Surachai Tonseeya*, Kanokphol Rochanakit*, Wasupon Wongvitvichot*, Uraiporn Masa-ard*, and Vorrada Loryuenyong*,**,†**

*Department of Materials Science and Engineering, Faculty of Engineering and Industrial Technology, Silpakorn University, Nakhon Pathom 73000, Thailand
**Center of Excellence on Petrochemical and Materials Technology, Chulalongkorn University, Bangkok 10330, Thailand
(*Received 7 May 2016 • accepted 11 August 2016*)

**Abstract**−We used a microwave heating system to increase *Jatropha* biodiesel yield, and to reduce both reaction time and energy consumption. The feasibility of converting natural and non-edible feedstocks including arcuate mussel shells and dolomitic rocks, into a novel high-performance, reusable, low-cost and heterogeneous catalyst for the synthesis of biodiesel was also explored. Arcuate mussel shells and dolomitic rocks were first ground and calcined at 900 °C for 2 h. After calcination, calcium oxide (CaO) or a mixed oxide of calcium and magnesium (CaO·MgO) was obtained as white powder, which was then chemically activated to improve the physical, chemical and surface properties, and catalytic activities of the catalysts. By heating CaO from waste shells in an excess dehydrated methanol under 65 °C at 8 h with nitrogen ($N_2$) flow, calcium methoxide ($Ca(OCH_3)_2$) catalyst was prepared. The CaO from natural rocks was, however, turned into calcium glyceroxide complex, by combining with methanol and glycerol of the by-product. It was determined that calcium glyceroxide ($Ca[O(OH)_2C_3H_5]_2$) was formed during the transesterification and acted as the most active phase. Catalyst characterization was by X-ray diffraction (XRD), X-ray fluorescence (XRF), scanning electron microscope (SEM), energy dispersive spectroscopy (EDS), Fourier transform infrared spectroscopy (FT-IR), and Brunauer-Emmett-Teller (BET) surface area and basic strength measurements. The reaction parameters, including reaction time, microwave power, methanol/oil molar ratio, catalyst dosage and catalyst reusability, were studied for fatty acid methyl esters (FAME) yield. The results indicated that $Ca(OCH_3)_2$ and $Ca[O(OH)_2C_3H_5]_2$ catalysts derived from waste shells and natural rocks showed good reusability, high energy efficient, environmental-friendly, low cost and facile route for the synthesis of biodiesel.

Keywords: Biodiesel, *Jatropha curcas* Oil, Waste Arcuate Mussel Shell, Dolomitic Rock, Microwave Heating System

## INTRODUCTION

Worldwide concern about the increase in carbon dioxide ($CO_2$) and other pollutants in the atmosphere as well as the declining reserves of crude oil has led to the development of alternative fuels. The renewable energy sources including solar, wind, ocean, hydropower, geothermal, and biomass have alternative sources of clean energy [1].

Biodiesel, consisting of fatty acid methyl esters (FAMEs), is a diesel replacement obtained from numerous renewable sources including animal fats, vegetable oils and used cooking oils. In comparison to petroleum-based diesel fuels, biodiesel is biodegradable, emits lower greenhouse gas (GHG), and does not produce particulate matter (PM) [2]. Biodiesel is normally derived from triglyceride (TG)-based feedstocks such as vegetable oil or animal fat by transesterification with methanol (methanolysis) under the catalytic condition to give the corresponding FAMEs and glycerol (by-product) [3]. This reaction is typically conducted using alkaline catalysts such as sodium hydroxide (NaOH) and potassium hydroxide (KOH), or potassium methoxide ($KOCH_3$), that are easily dissolved in the alcohol and are very active. However, the use of these homogeneous base catalysts raises some important disadvantages including high production costs and the environmental impact [4]. The removal of the homogeneous catalyst after reaction is also a main problem since aqueous quenching outcomes the formation of stable emulsions and saponification. The heterogeneous catalysts, on the other hands, can be easily separated from the reaction products with much more simplified product separation steps resulting in high yields of FAMEs and low catalyst cost due to catalyst regeneration. In addition, heterogeneous systems operate in both batch and continuous modes and are designed to give higher catalyst activity, selectivity and longer lifetimes, increasing the production capacities and lowering associated costs [5-8].

Among the heterogeneous basic catalysts, calcium oxide (CaO) is a potential candidate for its low cost, high basic strength, low methanol solubility, and environmental-friendly material. Generally, CaO could be derived from calcium carbonate ($CaCO_3$), which is the major constituent in many natural sources and wastes, such as eggshell, crab and shrimp shell, sea shell, fish scale, animal bone, coral, chalk and rock. Using biowastes as raw materials for prepa-

†To whom correspondence should be addressed.
E-mail: achanai130@gmail.com, vorrada@gmail.com

ration of CaO catalysts, could be produced the green catalysts with high cost effectiveness [9]. Due to its intrinsic pore structure in shell surface, the amount in abundance, and the main composition of $CaCO_3$, waste shell has been reported as a good raw material for the preparation of fine CaO powder [10,11]. Buasri et al. reported that the catalyst synthesized by waste shells could open the door for renewable energy and fuel, and at the same time reutilizes the waste generated [12]. Several works have improved the reaction rate by using modified CaO as solid basic catalysts [13].

Dolomite (dolomitic rock) is a natural mineral found all over the world. Chemically, it consists of a double carbonate of calcium ($CaCO_3$) and magnesium ($MgCO_3$) [14], and, therefore, can be used as a source of CaO and magnesium oxide (MgO) by calcination process [15]. Although pure MgO is not capable of catalyzing the transesterification by itself [3], these resultant CaO and MgO mixed phases exhibit good catalytic activity in the transesterification reaction due to the high basic characteristics [16].

Besides, CaO, calcium methoxide ($Ca(OCH_3)_2$) and calcium glyceroxide ($Ca[O(OH)_2C_3H_5]_2$) represent the potential alternative to heterogeneous alkaline catalysts in the transesterification of vegetable oil with methanol [4,5]. Liu et al. [17] reported a yield of 98% under the derived optimum conditions in the transesterification of soybean oil with methanol using $Ca(OCH_3)_2$ as solid catalyst. The catalyst continued its activity for 20 cycles in a reuse experiment with only slight decline in the yield of biodiesel [17]. Kouzu et al. [18] reported the transformation of $Ca[O(OH)_2C_3H_5]_2$ from CaO and $Ca(OCH_3)_2$ by combining with glycerol during methanolysis reaction. It presented the FAME yield produced by this heterogeneous catalyst is 95% [18]. Granados et al. [19] showed that the catalytic activity of CaO could be increased by creating $Ca[O(OH)_2C_3H_5]_2$ sites at the CaO surface [19]. Dissimilar synthetic strategies were applied to generate a large amount of $Ca[O(OH)_2C_3H_5]_2$ surface sites by the utilization of either diglycerides (DG), monoglycerides (MG) or glycerol [20,21].

Edible vegetable oils such as palm, sunflower and rapeseed oils are currently the source for biodiesel synthesis. This, however, leads to competition between the use of such feedstocks for food production and fuel production. Moreover, one of the major problems of biodiesel is its high cost of production, whereby 60-80% of the total biodiesel production cost is attributed to biodiesel feedstocks. Hence, the use of low-cost feedstock containing fatty acids is required to reduce the biodiesel production cost [21]. Development of low-value and non-edible vegetable oils for biodiesel production is a significant issue in the present and future research. The *Jatropha curcas* tree is a plant that can produce about 60% oil from the seed's kernel. Although *Jatropha Curcas* oil is not suitable for nutrition purposes without detoxification, it can be attractively used as the energy and fuel sources.

Microwave irradiation has been widely used as a productive method to extract oils from vegetable feedstock, biomass and animal fats. This method has many advantages in biodiesel production. It is cost effective and can be easily scaled-up. On average, the production cost by microwave heating is two-thirds less than that by conventional heating. In addition, it does not require samples to be devoid of water and has high reaction rate [22]. Previous studies indicated that microwave-assisted chemical reactions were better than those obtained using other synthetic techniques. It is more energy efficient, and can increase the reaction rate, product yields, and purity of products [23].

There are numerous studies focused on using a microwave heating system to improve the yields of biodiesel from *Jatropha curcas* oil. However, the *Jatropha*-derived biodiesel production using a microwave heating system and novel catalyst ($Ca(OCH_3)_2$ and $Ca[O(OH)_2C_3H_5]_2$ derived from waste arcuate mussel shell and dolomitic rock, respectively) has seldom been addressed. The effects of catalyst type, amount of catalyst, reaction time, molar ratio of methanol to oil, and microwave power are systematically studied. Moreover, the reusability and deactivation of the catalysts derived from the natural calcium materials were investigated.

## EXPERIMENTAL DETAILS

### 1. Materials

The arcuate mussel shell was collected as biowaste from Tae-lea Thai market, Samut Sakhon Province, Thailand. The waste shell was rinsed with running water to eliminate dust and impurities, and was then dried in an oven at 60 °C for 24 h. A natural dolomitic rock was donated from the L.S.M. (1999) Co. Ltd., Ratchaburi Province, Thailand. The *Jatropha Curcas* oil was purchased from Thai Physic Nut Oil Co. Ltd., Pathum Thani Province, Thailand. The molecular weight and density of the yellow oil were measured to be 870 g/mole and 0.817 g/cm$^3$, respectively. All chemicals were analytical-grade reagents (Merck, Darmstadt, Germany, >99% purity) and were used as received without further purification.

### 2. Preparation of $Ca(OCH_3)_2$ Catalyst from Waste Arcuate Mussel Shell

The dried arcuate mussel shell was crushed and sieved to pass 50-200 mesh screens (74-297 μm). The waste shell ($CaCO_3$) was calcined at 900 °C in air atmosphere with a heating rate of 10 °C/min for 2 h. The calcined sample (CaO) was obtained as white powder.

The $Ca(OCH_3)_2$ catalyst was prepared by heating CaO in an excess dehydrated methanol under reflux at 65 °C for 8 h with 50 mL/min nitrogen ($N_2$) flow. A constant stirring speed of 100 rpm was provided to facilitate sufficient contact between the reactants. After the reaction, the solid catalyst was filtered to remove the excess methanol and then dried in the vacuum oven at 105 °C for 1 h [24]. The product was kept in the closed vessel to avoid a reaction with $CO_2$ and humidity ($H_2O$) in air before being used.

### 3. Preparation of $Ca[O(OH)_2C_3H_5]_2$ Catalyst from Natural Dolomitic Rock

A natural dolomitic rock, calcium magnesium carbonate ($CaMg(CO_3)_2$), was ground in a mortar and sieved to reduce the particle sizes to less than 44 μm (mesh No. 325), followed by calcination in air using a muffle furnace from room temperature to the desired temperature (900 °C) at a heating rate of 10 °C/min and then held at this temperature for 2 h. A mixed oxide of calcium and magnesium (CaO·MgO), calcined material, was then cooled to room temperature in a desiccator.

$Ca[O(OH)_2C_3H_5]_2$ was synthesized as follows: the reactor was charged with 900 mL of methanol, 300 mL of glycerol and 20 g CaO·MgO calcined at 900 °C. The resulting mixture was vigorously stirred at 60 °C for 8 h. The mixture was cooled and centrifuged. The ob-

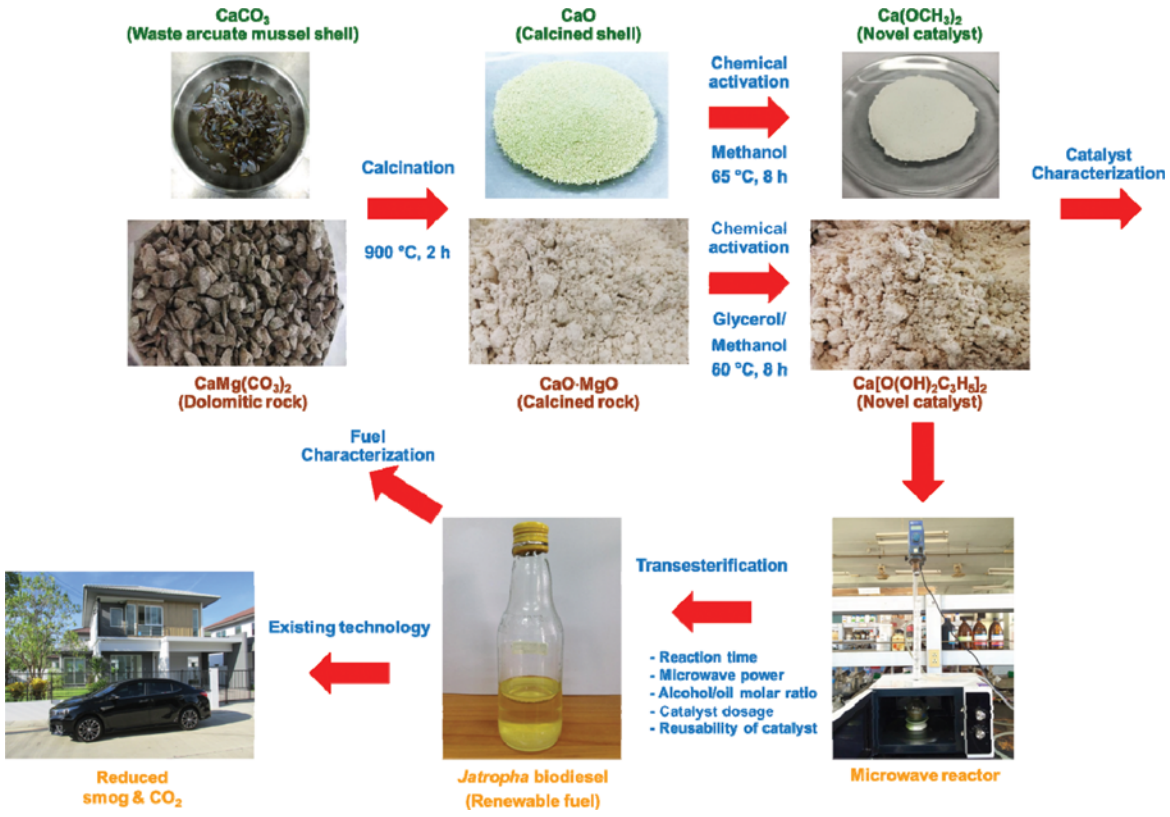


**Fig. 1. Preparation of novel catalysts derived from waste arcuate mussel shell and dolomitic rock for biodiesel production with a microwave reactor.**

tained precipitate was thoroughly washed with methanol and dried in oven at 100 °C for 2 h [25]. The novel catalyst was used in the transesterification reaction immediately. Fig. 1 shows the preparation process of natural material-derived catalyst.

**4. Characterization of Novel Catalysts**

X-ray diffraction (XRD) patterns of the powdered as-received, calcined and synthesized samples were obtained using a LabX XRD-6100, Shimadzu (Japan) analyzer operating at 30 kV and 20 mA with a Cu anode and a graphite monochromator ($\lambda$=1.5405 Å), an angle of scanning range 5-75° ($2\theta$), a scan step size of 0.04° and a scan rate of 2°/min. Energy dispersive X-ray fluorescence (XRF) spectrometer (model ED-2000, Oxford, England) was used to determine the element composition of the catalyst.

Scanning electron microscopy (SEM) was performed to investigate the surface morphology of the prepared catalyst by Hitachi TM3030 (USA) equipped with an energy dispersive spectroscope (EDS) at an accelerating voltage of 15 kV and working distance of 14-15 mm. The EDS was used to determine the element composition of manually chosen areas in the sample. For SEM analysis, the sample was coated with Au (gold) by using a sputter coater for protecting the induction of the electric current.

A Fourier transform infrared (FT-IR) spectrometer (Model: Bruker Optics, Vertex70, Germany) was used to identify the surface functional group of the catalyst at room temperature. Each spectrum was an average of 128 scans analyzed over the scanning over a wavelength of 500-4,000 $cm^{-1}$ at a resolution of 4 $cm^{-1}$. The samples were prepared by mixing a small amount of KBr and pressing them in the form of disks.

The surface area, mean pore diameter and pore volume of the catalysts were determined using a Quantachrome Instrument (Autosorb-1 Model No. ASIMP.VP4, USA) based on the $N_2$ adsorption-desorption method at 77 K. Prior to the analysis, all samples were degassed at 300 °C for 4 h to desorb the volatiles (if any) from the surface. A residual pressure of 300 μm Hg for 24 h was achieved via the degas port. The surface area was calculated using the Brunauer-Emmett-Teller (BET) equation, and the mean pore diameter and pore volume was obtained by applying the Barret-Joyner-Halenda (BJH) method on the desorption branch [9,26]. The basic strength of the synthesized catalysts was characterized using the Hammett indicators method as described at [4].

**5. The Procedure for the Synthesis of Biodiesel from *Jatropha curcas* Oil**

Production of biodiesel by transesterification of *Jatropha curcas* oil over $Ca(OCH_3)_2$ and $Ca[O(OH)_2C_3H_5]_2$ catalysts (Eq. (1)), was performed using a 100 mL three-neck round bottom flask equipped with a water-cooled reflux condenser and a mechanical stirrer (200 rpm) at atmospheric pressure, placed inside a household microwave oven (Samsung, Korea). The fixed 50 g of *Jatropha curcas* oil and the desired amount of the derived catalysts (1-5 wt%) were added to the glass reactor, and then the methanol was introduced to the vegetable oil at various methanol/oil molar ratios of 6 : 1-21 : 1. The reaction was operated at 200-800 W with varied reaction time of 1-5 min under a microwave heating system, and it was instantly stopped by rapid cooling in an ice bath [27].

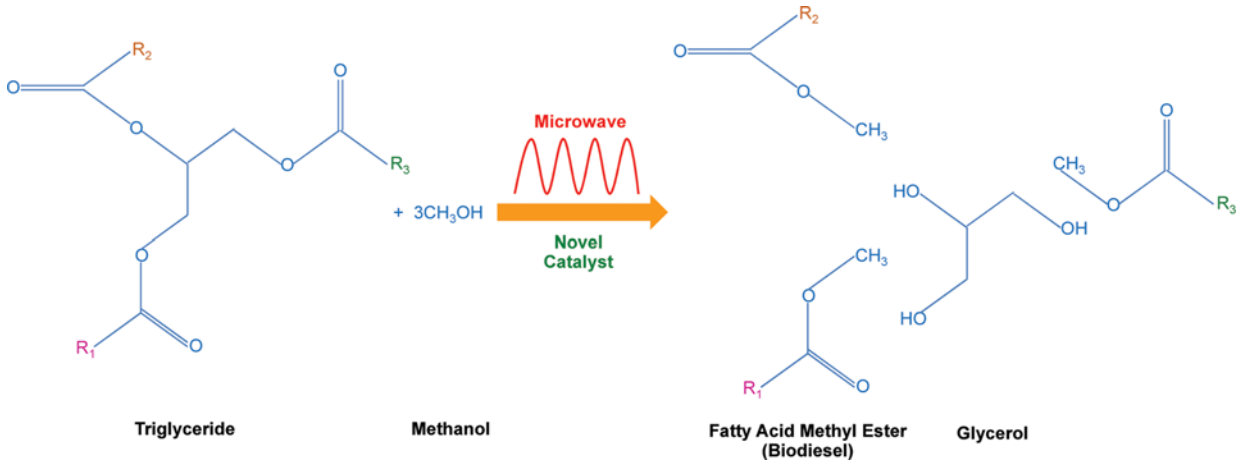


(1)

Once the reaction had finished, the mixture was then cooled to room temperature. After cooling, the catalyst was separated via centrifugation and the residual glycerol of the by-product was eliminated by washing with n-hexane and methanol. The mixture of FAME and glycerol was then transferred to a 250 mL separating funnel and allowed to stand at room temperature for 24 h [28]. The bottom layer (glycerol) was drained out and the upper layer, consisting of biodiesel (FAME), was collected carefully. Finally, the biodiesel was dried at 80 °C in a vacuum oven for 24 h and stored in an air-tight bottle for further investigations. All experiments were repeated three times and the standard deviation was never higher than 7% for any point.

The compositions of products were analyzed by gas chromatography - mass spectrometry (GC-MS, QP2010 Plus, Shimadzu Corporation, Japan) equipped with a flame ionization detector and a capillary GC column (DB-WAX, Carbowax 20M, 30 m×0.32 mm×0.25 μm) using the inner standard method as described by Granados et al. [29]. The yield of *Jatropha* biodiesel was calculated by dividing the weight of biodiesel with the weight of oil and multiplying the resulting number by 100 (Eq. (2)) [30].

$$\text{Yield (\%)} = \frac{\text{Weight of biodiesel}}{\text{Weight of raw oil}} \times 100 \quad (2)$$

The fuel properties, such as kinematic viscosity, density, flash point, cloud point, pour point, acid value, moisture content, ester content, free glycerin, total glycerin, iodine number, cetane number and calorific value of the *Jatropha* biodiesel, were measured following the ASTM standard methods. The obtained values were then compared with the United States biodiesel standard (ASTM D-6751) and European biodiesel standard (EN 14214).

### 6. Reuse of Solid Catalyst

An important characteristic feature of a catalyst is its "reuse" property [16]. The activated catalyst was used in reaction cycles under optimized conditions, and its catalytic activity was evaluated after every reaction cycle. The catalysts were used during seven cycles (1st run, 2nd run, 3rd run, 4th run, 5th run, 6th run and 7th run). In each cycle, the catalyst was separated from reaction medium via centrifugation, washed twice with n-hexane and methanol, and dried at 60 °C during 24 h and stored in a dessicator until the reaction. This procedure was followed for each reaction cycle.

Additionally, atomic absorption spectroscopy (AAS) elemental analysis was used to investigate the leached active calcium component ($Ca^{2+}$) in the methanol solution and FAME produced.

## RESULTS AND DISCUSSION

### 1. Catalyst Characterization

The XRD patterns of the catalyst from waste arcuate mussel shell obtained after calcination and synthesis reaction are demonstrated in Fig. 2. The natural waste shell mainly consisted of $CaCO_3$ phase, and after being calcined at 900 °C for 2 h, this $CaCO_3$ was completely converted to CaO by evolving the $CO_2$ [31]. The very appreciable narrow and intense peaks of calcined waste shell at $2\theta$=32 and 37° were attributed to (1 1 1) and (2 0 0) orientations of CaO phase, as shown in Fig. 2(b). This result defines the high crystallinity of the CaO catalyst [27,32,33]. After reacting with methanol under reflux, this CaO was transformed into $Ca(OCH_3)_2$, as is evident from the characteristic peak of $Ca(OCH_3)_2$ at $2\theta$=11° in Fig. 2(c). Similar results were reported in earlier studies [34]. The

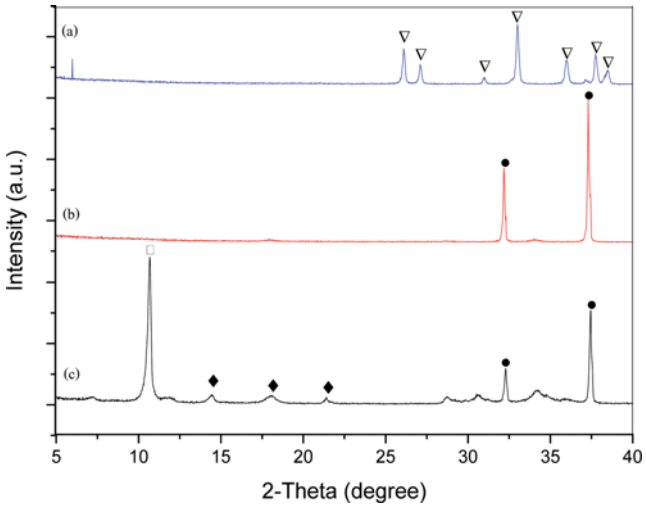


**Fig. 2. XRD patterns of (a) waste arcuate mussel shell, (b) calcined shell, and (c) novel catalyst (▽: $CaCO_3$, ●: CaO, □: Ca $(OCH_3)_2$, and ◆: $Ca(OH)_2$).**

products also consisted of unreacted CaO and calcium hydroxide ($Ca(OH)_2$), which had possibly appeared due to the interaction of catalyst with water [24,35].

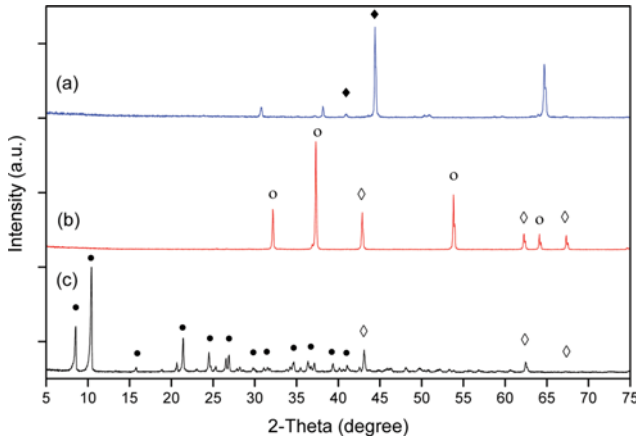


**Fig. 3. XRD patterns of (a) natural dolomitic rock, (b) calcined rock, and (c) novel catalyst (□: $CaCO_3$, ◆: $MgCO_3$, ○: CaO, ◇: MgO, and ●: $Ca[O(OH)_2C_3H_5]_2$).**

Fig. 3 illustrates the XRD patterns of both natural dolomite and calcined dolomite. Raw dolomite rock exhibited several diffraction peaks located at $2\theta$=33°, 37°, 41°, 44°, 50° and 65°, which were attributed to dolomite phase, $CaMg(CO_3)_2$ [16]. After being calcined at 900 °C for 2 h, the diffraction peaks from carbonate species disappeared due to their decomposition into the oxide and $CO_2$ gas upon heating. The diffraction peaks located at $2\theta$=32°, 37°, 53° and 64° were assigned to lime (CaO), and those at $2\theta$=42° and 62° were attributed to periclase (MgO) [3]. The characteristic peaks at $2\theta$=8°, 10°, 21°, 24°, 26°, 34° and 36° were matched to the diffraction pattern of the reacted rock, so-called Ca-glyceroxide ($Ca[O(OH)_2C_3H_5]_2$) [4] as a by-product from the reaction of CaO with glycerol. The structure of this compound is formed by tetramers ($Ca_4[O(OH)_2C_3H_5]_8$) held together by a complex hydrogen-bond network [20].

The elemental compositions of prepared catalysts were evaluated using XRF, as illustrated in Table 1. Calcium (Ca) was the major element presented in arcuate mussel shell and constitutes more than 97 wt% of the total catalyst. This indicated that the shell was mostly composed of calcium compounds such as CaO and $Ca(OCH_3)_2$ upon calcination and chemical activation. The dolomitic rock, on the other hand, had Ca and magnesium (Mg) as

**Table 1. Elemental compositions (wt%) of catalysts determined by XRF analysis**

| Natural material-derived catalyst | Ca | Mg | Si | S | Al | Others |
|---|---|---|---|---|---|---|
| Arcuate mussel shell (calcined and treated) | 97.63 | 0.18 | 0.15 | 0.62 | 0.05 | 1.37 |
| Dolomitic rock (calcined and treated) | 68.96 | 28.92 | 0.70 | 0.35 | 0.34 | 0.73 |

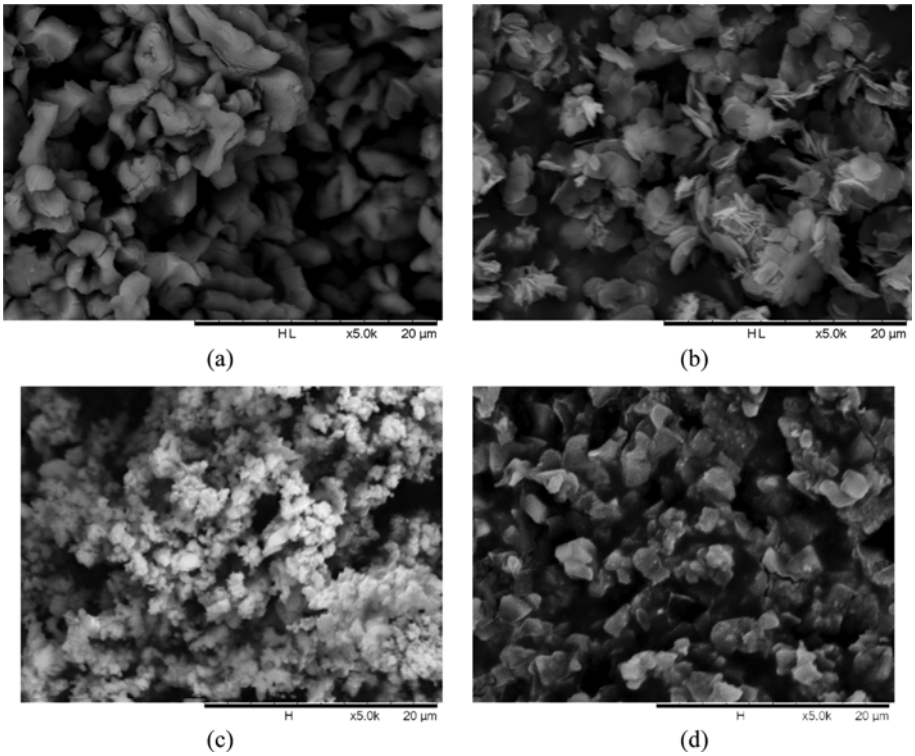


**Fig. 4. SEM micrographs of (a) CaO, (b) $Ca(OCH_3)_2$, (c) CaO·MgO and (d) $Ca[O(OH)_2C_3H_5]_2$ catalysts. Images are magnified at 5000×, and scale bars represent 20 µm.**

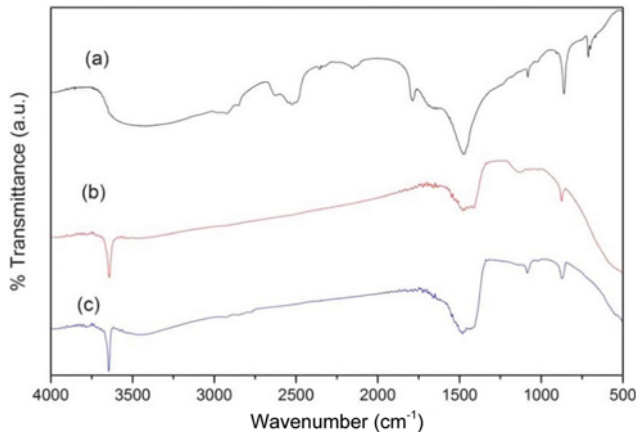


**Fig. 5. FT-IR spectra of (a) waste arcuate mussel shell, (b) calcined shell, and (c) novel catalyst.**

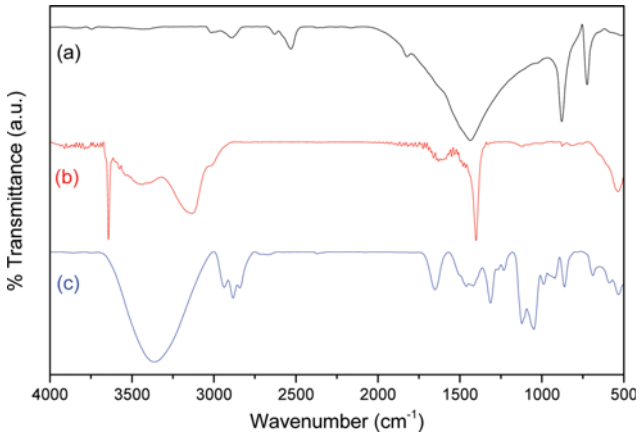


**Fig. 6. FT-IR spectra of (a) natural dolomitic rock, (b) calcined rock, and (c) novel catalyst.**

the major elements more than 68% and 28% of the total catalyst, respectively. Other elements appeared in minor amounts.

Fig. 4 shows the morphology of the calcined waste shell (CaO) and synthesized catalyst ($Ca(OCH_3)_2$). As can be seen, the SEM image of CaO shows compact and irregular particles, while that of flower-like and plate-like particles was observed in $Ca(OCH_3)_2$ catalyst. This result was similar to that reported by Kouzu et al. [34]. In addition, a large number of pores are visible on the surface of the catalysts, which contributed to the high surface area of catalyst [36]. For dolomite sample, the change in the external morphology occurred during the calcination and is illustrated in Fig. 4(c). Starting with large particles and a smooth surface of dolomite, calcination at 900 °C changed this surface by making it rougher and decreasing the particle size. Simultaneously, the surface area and the pore volume of the samples increased significantly. This increase in surface area upon calcination was attributed to the formation of pores due to the expulsion of $CO_2$ [37]. Fig. 4(d) shows an SEM image of particles of tablet shape $Ca[O(OH)_2C_3H_5]_2$ with sizes ranging between 1 and 5 μm [20].

The typical FTIR spectra of waste arcuate mussel shell, calcined shell and novel catalyst are given in Fig. 5. For waste shell, the characteristic peaks of C-O stretching and bending modes of $CaCO_3$ were observed at 3,122, 2,508, 1,475 and 869 $cm^{-1}$. During the calcination process, $CaCO_3$ decomposed into CaO and $CO_2$. A new peak appeared at 3,644 $cm^{-1}$, indicating the formation of basic OH groups attached to the calcium atoms [10]. After reacting with methanol under reflux, important features appeared including the -C-O stretching vibration of primary alcohol (1,090 $cm^{-1}$), -OH stretching vibration of primary alcohol (3,647 $cm^{-1}$), and -C-H alkene bending (1,479 $cm^{-1}$) [21].

The FTIR spectra of the natural dolomitic rock, calcined rock and novel catalyst are shown in Fig. 6. For dolomite mineral, there were three characteristic peaks of the out-of-plane bending and the asymmetric stretching modes of the carbonate groups located at 878, 1,436 and 726 $cm^{-1}$, respectively. After thermal treatment, a new hydroxyl band appeared at 3,643 $cm^{-1}$, which can be assigned to -OH groups attached to the CaO and MgO. The band at 1,629 and 1,401 $cm^{-1}$ can be assigned to the symmetric and asymmetric stretching vibrations of O-C-O bonds of unidentate carbonate at the surface of CaO·MgO. The band centered at 3,453 $cm^{-1}$ was assigned to H-bonded water [16]. Fig. 6(c) illustrates FTIR spectra of catalyst. The band at 3,364 $cm^{-1}$ can be attributed to the OH stretching vibration of the C-OH group of calcium glyceroxide bonded to the calcium atoms. The bands at 2,937, 2,883 and 2,842 $cm^{-1}$ are related to the C-H stretching. Various bands of C-H bending modes (1,419, 1,232, 1,049 and 988 $cm^{-1}$), C-O-H bending modes (1,312 $cm^{-1}$) and C-O stretching mode (1,121 $cm^{-1}$) of $Ca[O(OH)_2C_3H_5]_2$ were also observed [38].

EDS analysis on the surface of $Ca(OCH_3)_2$ catalyst was performed, and the spectra are shown in Fig. 7(a). The atomic percent (at%) of calcium (Ca), oxygen (O) and carbon (C) on a particular area at the surface of synthesized catalyst was determined to be 19.71%, 65.49% and 14.80%, respectively. The atomic ratio between calcium and oxygen (Ca:O) was 3.32, while the atomic ratio between calcium and carbon (Ca:C) was 1.33. Peaks at 2.3 keV and 4.0 keV represent the sputter coating of gold/platinum, and the values were excluded from the final results. The surface of catalyst has strong basic character and therefore has a tendency to absorb moisture. The peaks attributed to -OH on the XRD result explain the presence of more oxygen atoms on the surface. Furthermore, $CO_2$ adsorbed within the pores on the basic catalyst surface has an influence on both Ca:O and Ca:C. Hydrogen was not quantified by EDS because of small orbital diameter (atomic number=1), which reduced the catch probability for spectroscopy to almost zero [24]. Another important and useful capability of the EDS technique is x-ray mapping of elements. Here, the positions of specific elements emitting characteristic x-rays within an inspection field can be indicated by a unique color. In Fig. 7(b) the map of Ca, Mg, C and O is shown overlaid with the original image. When chemical mapping is performed, it reveals that in the $Ca[O(OH)_2C_3H_5]_2$ catalyst, Ca, C and O are concentrated on specific areas, most probably those where Mg is found. This was also confirmed in the EDS chemical mapping, which showed that 12.82% of the Mg could be identified.

The BET specific surface area ($S_{BET}$), average pore diameter ($D_p$) and total pore volume ($V_p$) are important characteristics of solid

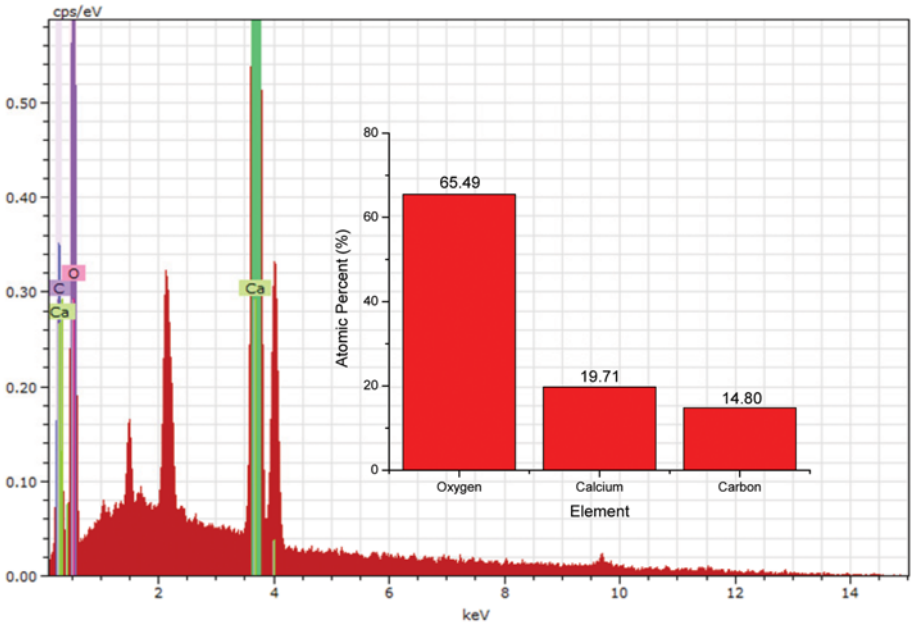


(a)

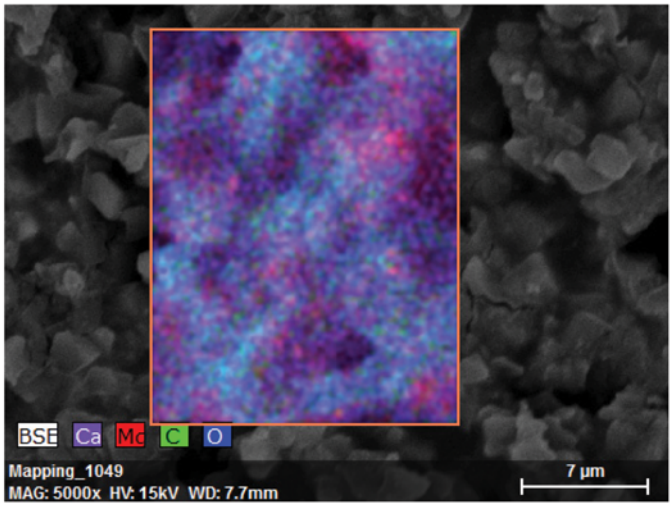


(b)

**Fig. 7. EDS (a) spectra on surface of $Ca(OCH_3)_2$ catalyst, and (b) chemical mapping of $Ca[O(OH)_2C_3H_5]_2$ catalyst for Ca, Mg, C and O.**

**Table 2. $S_{BET}$, $D_p$, $V_p$ and basic strength of catalysts**

| Natural naterial-derived catalyst | $S_{BET}$ ($m^2$/g) | $D_p$ (nm) | $V_p$ ($cm^3$/g) | Basic strength (H_) | Reference |
|---|---|---|---|---|---|
| Arcuate mussel shell (calcined and treated) | 31.24 | 31.88 | 0.20 | 15.0<(H_)<18.0 | This work |
| Dolomitic rock (calcined and treated) | 39.26 | 38.92 | 0.44 | 15.0<(H_)<18.4 | This work |
| Crab (*Scylla serrata*) shell (calcined) | 14.2 | - | - | 15.0<(H_)<18.4 | [40] |
| Cockle (*Anadara granosa*) shell (calcined) | 11.4 | - | - | 15.0<(H_)<18.4 | [40] |
| Natural dolomite (calcined) | 21.4 | - | 0.25 | 15.0<(H_)<18.0 | [37] |
| Natural dolomite (calcined and treated) | 39.2 | - | 0.44 | 15.0<(H_)<18.0 | [37] |

catalyst because they are closely related to the catalytic activity. In general, the reactivity is directly proportional to the external surface area of catalyst [17]. Table 2 shows the analyzed results of novel catalysts. It indicated that the $Ca(OCH_3)_2$ catalyst had a surface area of 31.24 $m^2$/g, an average pore diameter of 31.88 nm and a total pore volume of 0.20 $cm^3$/g. In comparison to previous work, this suggested that the $Ca(OCH_3)_2$ catalyst was favorable to be used in the liquid phase reaction, since it provided sufficient active sites in stirrer type reactor [36]. The calcination and chemical activation of the as-received dolomitic rock at 900 °C for 2 h increased

the surface area and total pore volume. The average pore size of the $Ca[O(OH)_2C_3H_5]_2$ catalyst was 1.22 times bigger than that of the $Ca(OCH_3)_2$ catalyst, suggesting that the particles of the calcined and treated arcuate mussel shell were packed much closer. Presumably, the presence of the MgO in the calcined and treated dolomitic rock prevented the sintering of CaO crystallites, since the melting point of MgO (2,852 °C) is higher than that for CaO (2,613 °C) [39]. The basic strength (H_) of the solid catalyst was determined by a method based on the color change of Hammett indicators. If the indicator exhibited a color change, then the catalyst was labeled as stronger than the indicator, and if not, then the catalyst was said to be weaker than the indicator [40]. The basic strength and basicity are the most important properties regarding their application as a catalyst for the transesterification of TG [4]. The reaction activity depends on the number of basic sites present in the catalysts as well as on their strength [41]. In this study, the basic strength, physical and surface properties of novel catalysts are within the range reported by other researchers.

**2. Catalytic Testing**

The activities of the catalysts were studied by investigating the effects of reaction time, power of microwave, molar ratio of methanol to oil, catalyst dosage and reusability of catalyst in the transesterification. For the following experiments, calcined and treated arcuate mussel shell and dolomitic rock were used as novel catalysts to catalyze the microwave-assisted reaction of *Jatropha curcas* oil and methanol.

2-1. Effect of Reaction Time

The reaction time is an important reaction parameter, which is closely related with energy cost of the biodiesel production process. As shown in Fig. 8, the results revealed that the conversion of *Jatropha curcas* oil was comparatively low at a shorter reaction time (1-2 min) due to the presence of the heterogeneous mass transfer systems of the catalyst [21]. The FAME yield was increased significantly and reached about 98.25 and 98.97% after 3 min of reaction at 600 W for $Ca(OCH_3)_2$ and $Ca[O(OH)_2C_3H_5]_2$ catalyst, respectively. With a further increase in reaction time, FAME yield did not increase significantly, and was almost constant at about 98% between 3 min and 6 min of reaction time. Similar results were obtained by Ilgen [41]. The suitable reaction time required for obtaining the highest amount of methyl ester (ME) was, therefore, 3 min.

The FAME yield obtained depended on the reaction time over the calcined and treated arcuate mussel shell or dolomitic rock catalysts. The conversion of TG occurred at a higher rate when using the $Ca[O(OH)_2C_3H_5]_2$ as the catalyst, which was due to its higher basicity. In addition, the catalyst derived from dolomite rock had smaller CaO crystallites than that from the waste shell, which was probably due to the presence of the MgO dispersed in the CaO matrix of the calcined dolomite. The formation of a mixed CaO·MgO in the calcined dolomite maintained the catalyst morphology, while a sintering effect was observed for the pure CaO in the calcined waste shell [39]. Consequentially, the $Ca[O(OH)_2C_3H_5]_2$ catalyst gave a higher methanolysis rate than $Ca(OCH_3)_2$ catalyst.

Moreover, the reaction time was reduced substantially when microwave heating was used. The highly effective transesterification process in a microwave heating system was attributed to the direct adsorption of radiation by the OH group of the reactant. The OH group was directly excited by the microwave radiation, causing the local temperature surrounding the OH group to be much higher than that of the environment; once the activation energy considerably exceeded the amount required for transesterification, the reaction occurred. Therefore, the microwave heating system offers more favorable performance, process simplicity, and energy efficiency than conventional heating system in biodiesel production [42].

2-2. Effect of Microwave Power

To determine the optimum parametric conditions for the production of biodiesel assisted by a microwave heating system, the effect of power supplied by the microwave oven was studied. The experiments were conducted on the *Jatropha curcas* oil at 12 : 1 methanol/oil molar ratio with a supplied energy of 200-800 W for 3 min and catalyst dosage of 3 wt%. The FAME yield results shown in Fig. 9 elucidated the effect of microwave power at 200 W (54.23% and 61.87%), 300 W (66.58% and 73.83%), 450 W (78.84% and 81.64%), and 600 W (98.25% and 98.97%) for $Ca(OCH_3)_2$ and $Ca[O(OH)_2C_3H_5]_2$ catalyst, respectively. They were clear that higher

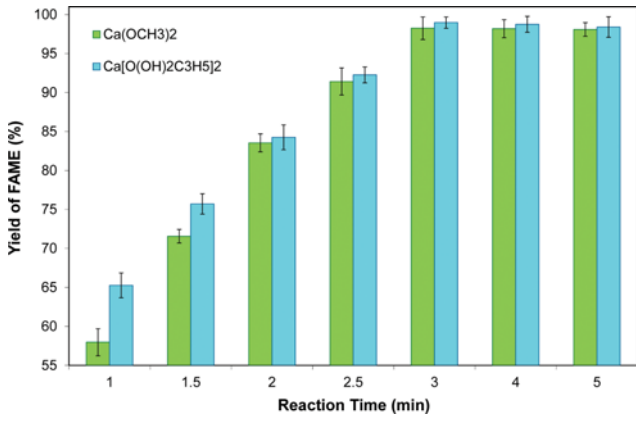


**Fig. 8. Effect of reaction time on the FAME yield. Reaction conditions: microwave power of 600 W; methanol/oil molar ratio of 12 : 1; and catalyst dosage of 3 wt%.**

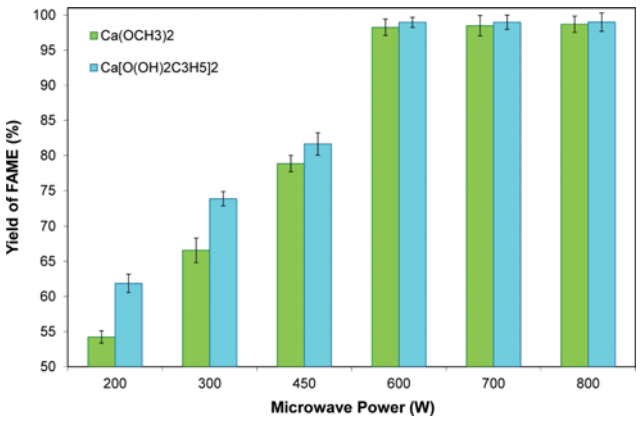


**Fig. 9. Effect of microwave power on the FAME yield. Reaction conditions: reaction time of 3 min; methanol/oil molar ratio of 12 : 1; and catalyst dosage of 3 wt%.**

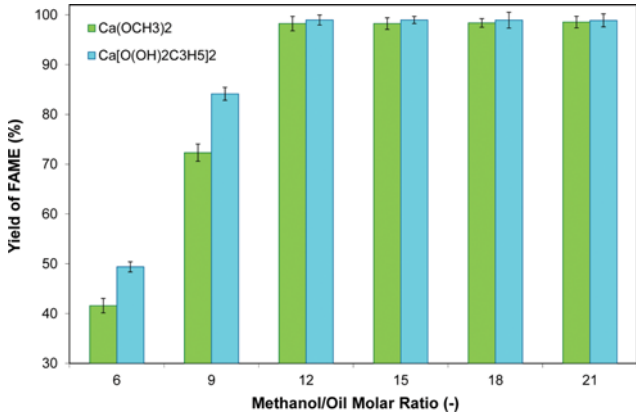


**Fig. 10. Effect of methanol/oil molar ratio on the FAME yield. Reaction conditions: reaction time of 3 min; microwave power of 600 W; and catalyst dosage of 3 wt%.**

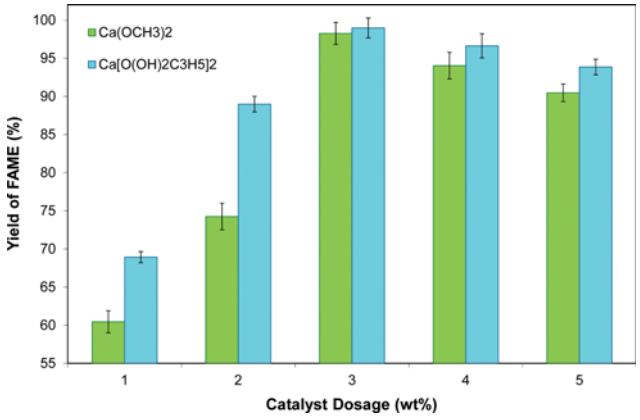


**Fig. 11. Effect of catalyst dosage on the FAME yield. Reaction conditions: reaction time of 3 min; microwave power of 600 W; and methanol/oil molar ratio of 12 : 1.**

microwave power gave rise to higher biodiesel yield. It was considered that the related chemical reactions were accelerated by microwave energy, giving rise to intense localized heating, and thereby accelerating the chemical reaction and giving high product yields in a short time [43]. Similar results were found in earlier works [44,45]. With the maximum yield achieved, the microwave power of 600 W would be chosen for further investigation. However, the microwave output must not be too high, as it may cause damage to organic molecules such as TG, which are cleaved to free fatty acid (FFA). These results suggest that appropriate power dissipation control will result in effective use of microwave energy and reduce energy requirements [45].

2-3. Effect of Methanol/Oil Molar Ratio

The molar ratio of methanol to oil is one of the important factors that affect the FAME production. Theoretical minimum methanol/oil molar ratio should be 3 : 1 for the complete conversion of oil to biodiesel. Nevertheless, a higher molar ratio is required to get the desired conversion. The evaluation of FAME yield from *Jatropha curcas* oil over $Ca(OCH_3)_2$ and $Ca[O(OH)_2C_3H_5]_2$ catalysts as a function of methanol/oil molar ratio (6 : 1-21 : 1) at 800 W for 3 min is presented in Fig. 10. FAME yield was very low (less than 50%), when a low molar ratio of methanol/oil as 6 : 1 was used. The lower methanol/oil ratios resulted in poor suspension of the slurry in the reacting solution, which possibly induced mass transfer problems, and thus resulted in lower activity. In accordance with reported literature [27], the activity steadily increased with higher methanol/oil molar ratios. The maximum biodiesel production was achieved at molar ratio of 12 : 1. For methanol/oil molar ratios greater than 12 : 1, further increase in the FAME yield was negligible. Excess methanol was required not only to shift the equilibrium toward and forward direction, but also to wash away the product molecules from the catalyst surface to regenerate the active sites. Nonetheless, polar OH group from methanol would cause emulsification, which resulted in difficulty in separation of FAME and glycerol [1]. Therefore, 12 : 1 was the appropriate methanol/oil molar ratio for this reaction.

2-4. Effect of Catalyst Dosage

The effect of novel catalyst concentration on the transesterification was investigated with the catalyst dosage varying from 1 wt% to 5 wt% (weight to oil) at 800 W for 3 min with methanol/oil molar ratio of 12 : 1. From Fig. 11, in the absence of solid catalyst, there was no FAME formed in the reaction. It could be found that low concentration of catalyst was insufficient to catalyze the reaction for completion, and by increasing the amount of catalyst, an enhancement of the FAME yield was obtained. The results indicated that a high concentration of catalyst facilitates to increase the total number of available active catalytic sites for the reaction. Hence, the rate of reaction could be increased. Teo et al. [21] reported that the mesoporous properties of catalyst could be an effective catalyst for the reaction to take place at the internal surface by adsorbing large organic molecules into the uniform pore structure [21]. Meanwhile, macropore structures of the catalyst provided a large external surface that acts as the active site for rapid mass transfer. The maximum FAME yield of 98.25% and 98.97% was obtained with the $Ca(OCH_3)_2$ and $Ca[O(OH)_2C_3H_5]_2$ catalyst loading of 3 wt%, respectively. No further enhancement of FAME yield was gained as excessive catalyst was employed. This decreasing trend was due to the saponification in the presence of high amount of catalysts, which increased the viscosity of the reactants and lowered the yield of FAME, as suggested by Tang et al. [13]. This result implied that the transesterification of TG was strongly dependent on the number of basic sites. Therefore, the 3 wt% calcined and treated arcuate mussel shell and dolomitic rock was the optimal catalyst amount in this reaction.

2-5. Stability and Reusability of Catalyst

Besides activity, another critical point to examine is the catalyst activity loss and reusability. One of the main disadvantages of homogeneous catalysts is that they cannot be recovered. So, in the present study, we evaluated the catalyst to study its efficiency and reusability. The catalyst was recycled to test its activity as well as stability. After being used, the catalyst was separated from the reaction mixture by filtration, washed with methanol to remove any adsorbed stains, and then dried at 80 °C in an oven for 12 h. Catalysts from different reactions was recovered following the above procedure [46]. The recovered catalyst was charged for the subsequent run. After each run, catalyst was collected quantitatively, and

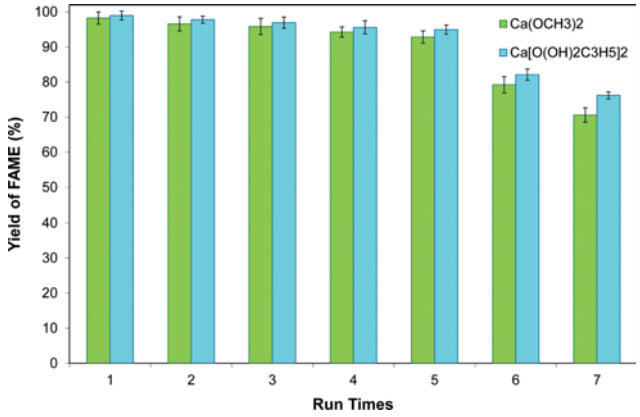


**Fig. 12. Effect of reusability of catalyst on the FAME yield. Reaction conditions: reaction time of 3 min; microwave power of 600 W; methanol/oil molar ratio of 12 : 1; and catalyst dosage of 3 wt%.**

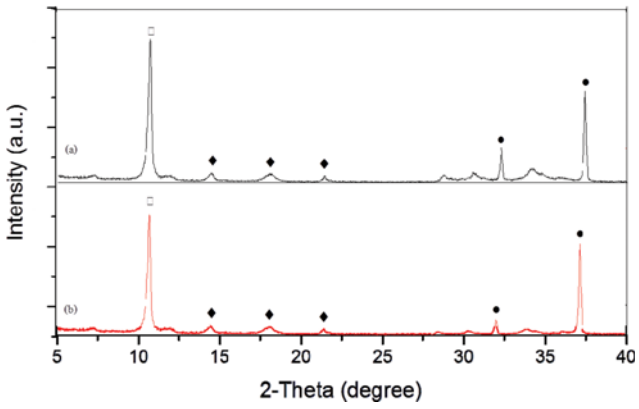


**Fig. 13. XRD patterns of (a) fresh and (b) recycled catalysts derived from waste arcuate mussel shell (●: CaO, □: $Ca(OCH_3)_2$, and ◆: $Ca(OH)_2$).**

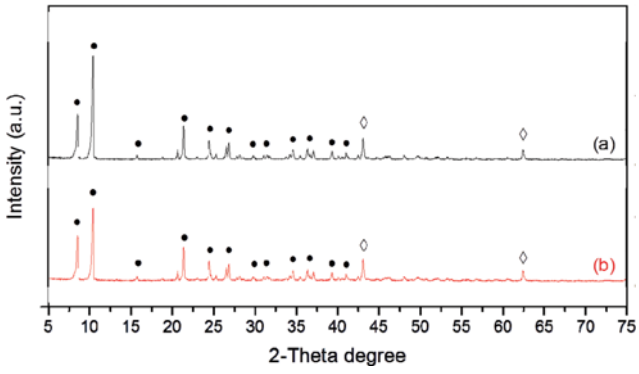


**Fig. 14. XRD patterns of (a) fresh and (b) recycled catalysts derived from dolomitic rock (●: $Ca[O(OH)_2C_3H_5]_2$, and ◇: MgO).**

the same procedure was carried out to recover the catalyst after each cycle.

Catalyst recycling is an important step as it minimizes the process cost. Previous studies demonstrated that heterogeneous catalyst could be recycled and have been proven to have good recyclability [47]. To check the catalyst reusability, the used catalyst was retested at the following condition: a 3 wt% catalyst dosage at 12 : 1 methanol/oil molar ratio with a supplied energy of 600 W for 3 min. The results of the recycling studies conducted on *Jatropha curcas* oil are summarized in Fig. 12. It was found that the $Ca(OCH_3)_2$ and $Ca[O(OH)_2C_3H_5]_2$ catalysts could be reused up to five times, and the FAME yield was around 98.97-92.86%. The structural/phase changes of fresh and recycled catalysts (five times) were observed by XRD technique (Figs. 13 and 14). The XRD patterns of the recycled catalysts derived from waste arcuate mussel shell and dolomitic rock have shown slight decreasing and shifting of some peaks. In addition, a significant drop in biodiesel yields (70.61% and 76.21% for $Ca(OCH_3)_2$ and $Ca[O(OH)_2C_3H_5]_2$ catalyst, respectively) was observed while reusing the catalyst for the 7th run. According to these results, after each recycle, the catalyst appeared to have lost some activity, indicating that there was some small degree of active calcium species ($Ca^{2+}$) leaching from the catalyst, and, hence, minor deactivation. The catalyst loss during the recovery and transferring process was less than 3% in each repetition, and so did not account for this deactivation behavior. The deactivation of the catalyst could be due to calcium leaching and the

**Table 3. The reusability comparison between natural material-derived catalysts**

| Natural material-derived catalyst | Reaction condition | | | | | | Reference |
|---|---|---|---|---|---|---|---|
| | Feedstock | Catalyst dosage (wt%) | Methanol/ oil molar ratio | Reaction time | Run | Yield (Y) or conversion (C) | |
| Arcuate mussel shell | *Jatropha curcas* oil | 3 | 12 : 1 | 3 min (microwave) | 5 | 92.86% (Y) | This work |
| Dolomitic rock | *Jatropha curcas* oil | 3 | 12 : 1 | 3 min (microwave) | 5 | 94.95% (Y) | This work |
| Industrial eggshell waste | Palm oil | 10 | 18 : 1 | 4 min (microwave) | 5 | 83.37% (Y) | [43] |
| Oyster shell | *Jatropha curcas* oil | 4 | 15 : 1 | 5 min (microwave) | 3 | 76.86% (Y) | [27] |
| *Pyramidella* shell | *Jatropha curcas* oil | 4 | 15 : 1 | 5 min (microwave) | 3 | 80.95% (Y) | [27] |
| *Pomacea* sp. shell | Palm oil | 4 | 7 : 1 | 4 h (conventional) | 3 | 95.61% (Y) | [10] |
| Waste animal bone | Palm oil | 20 | 18 : 1 | 4 h (conventional) | 5 | 83.70% (C) | [49] |
| Chicken bone | Waste cooking oil | 5 | 15 : 1 | 4 h (conventional) | 6 | 57.64% (Y) | [50] |
| Natural dolomite | Palm oil | 10 | 30 : 1 | 3 h (conventional) | 3 | 96.08% (Y) | [39] |
| Chicken eggshell | *Jatropha curcas* oil | 5 | 12 : 1 | 1 h (conventional) | 4 | 95.60% (C) | [51] |

**Table 4. The fuel properties of biodiesel obtained in the transesterification of *Jatropha curcas* oil**

| Fuel property | Natural material-derived catalyst | | ASTM D-6751 | EN 14214 |
|---|---|---|---|---|
| | Arcuate mussel shell | Dolomitic rock | | |
| Kinematic viscosity ($mm^2/s$) @ 40 °C | 4.4 | 4.3 | 1.9-6.0 | 3.50-5.00 |
| Density ($kg/m^3$) @ 15 °C | 888 | 883 | 860-894 | 860-900 |
| Flash point (°C) | 165 | 169 | >130 | >120 |
| Cloud point (°C) | 12 | 11 | −3 to 12 | Not specified |
| Pour point (°C) | 9 | 8 | −15 to 10 | Not specified |
| Acid value (mg KOH/g oil) | 0.22 | 0.19 | ≤0.5 | <0.5 |
| Moisture content (%) | 0.01 | 0.01 | <0.05 | <0.05 |
| Ester content (%) | 98.25 | 98.97 | >96.5 | >96.5 |
| Free glycerine (%) | 0.008 | 0.009 | <0.02 | <0.02 |
| Total glycerine (%) | 0.12 | 0.11 | <0.24 | <0.24 |
| Iodine number (g $I_2$/100 g oil) | 116 | 115 | Not specified | <120 |
| Cetane number | 55 | 57 | >47 | >51 |
| Calorific value (MJ/kg) | 40.83 | 42.10 | Not specified | Not specified |

impurities that come from feedstock oil, such as moisture [35,38].

As shown in Table 3, the catalytic activities of novel catalysts were within the range reported by other researchers. These heterogeneous catalysts showed high stability and reusability for transesterification of *Jatropha curcas* oil with small loss of their catalytic activity during reaction. Small loss of the catalyst was an important factor for good catalyst reusability [48].

**3. Fuel Properties of Biodiesel**

To be used in diesel engines, biodiesel must meet various specifications stated in biodiesel standard, mainly United States biodiesel standard (ASTM D-6751) and European biodiesel standard (EN 14214) [9,52]. The fuel properties (kinematic viscosity, density, flash point, cloud point, pour point, acid value, moisture content, ester content, free glycerin, total glycerin, iodine number, cetane number and calorific value) of FAME obtained in this work are summarized in Table 4 along with a comparison to the recommended biodiesel international standards ASTM D-6751 and EN 14214. Most of its properties are in the range of fuel properties as described in the latest standards for biodiesel. In addition, the energy efficiency for *Jatropha* biodiesel production by using novel catalysts was calculated (in Appendix A) and found to be more efficient (16.98 MJ/MJ and 17.07 MJ/MJ for $Ca(OCH_3)_2$ and $Ca[O(OH)_2C_3H_5]_2$ catalyst, respectively) than that of commercial CaO (15.51 MJ/MJ). However, the energy efficiency for the overall process from catalysts design to biodiesel production by using CaO catalyst was excellent, because the catalyst modification is an energy-intensive process.

## CONCLUSION

The present study demonstrates the successful application of calcined and treated arcuate mussel shell and dolomitic rock as the efficient heterogeneous catalysts for transesterification of *Jatropha curcas* oil with methanol. After calcination at 900 °C for 2 h, the catalyst derived from natural rock had smaller CaO crystallites and a higher basicity than that from the waste shell, probably due to the presence of the MgO dispersed in the CaO matrix of the calcined dolomite. The highest FAME yields of 98.25% and 98.97% for $Ca(OCH_3)_2$ and $Ca[O(OH)_2C_3H_5]_2$ catalyst were obtained under the optimum condition (reaction time=3 min, microwave power=600 W, methanol/oil molar ratio=12 : 1, and catalyst dosage=3 wt%). The experimental results showed that the novel catalysts had excellent catalytic activity, stability, and reusability during the reaction. The solid catalysts were used for six cycles, and apparent low activity losses were observed. The reaction time was reduced significantly, and the yield of biodiesel was improved due to the use of microwave heating. This result confirmed that a microwave heating system could achieve better performance, in comparison to conventional heating system. The physical and chemical properties of biodiesel produced conformed to the available standards (ASTM D-6751 and EN 14214). Natural material is therefore a useful raw material for the production of a cost effective, high efficient, low toxicity, and green catalyst for transesterification.

## ACKNOWLEDGEMENTS

This work is supported by Silpakorn University Fund for Research and Creative Work (Faculty of Engineering and Industrial Technology) and Silpakorn University Research and Development Institute. The authors also wish to thank the Department of Materials Science and Engineering, Faculty of Engineering and Industrial Technology, Silpakorn University for supporting and encouraging this investigation.

## AUTHOR CONTRIBUTIONS

All the authors contributed to this work. Achanai Buasri designed the study, conceived the experiments, and wrote the first draft of the paper. Methasit Lukkanasiri, Raviporn Nernrimnong, Surachai Tonseeya, Kanokphol Rochanakit, Wasupon Wongvitvichot and Uraiporn Masa-ard performed the experiments in the laboratory. Vorrada Loryuenyong contributed to the conceptual approach, analyzed the data, helped in the discussion of results and thoroughly revised the paper.

## CONFLICT OF INTEREST

The authors declare no conflict of interest.

## ABBREVIATIONS

FAME : fatty acid methyl ester
ME : methyl ester
FFA : free fatty acid
TG : triglyceride
DG : diglyceride
MG : monoglyceride
GHG : greenhouse gas
PM : particulate matter
XRD : X-ray diffraction
XRF : X-ray fluorescence
SEM : scanning electron microscope
EDS : energy dispersive spectroscopy
FT-IR : fourier transform infrared spectroscopy
BET : Brunauer-Emmett-Teller
GC-MS : gas chromatography - mass spectrometry

## REFERENCES


1. S. H. Teo, U. Rashid and Y. H. Taufiq-Yap, *Fuel*, **136**, 244 (2014).
2. N. Degirmenbasi, S. Coskun, N. Boz and D. M. Kalyon, *Fuel*, **153**, 620 (2015).
3. S. L. Niu, M. J. Huo, C. M. Lu, M. Q. Liu and H. Li, *Bioresour. Technol.*, **158**, 74 (2014).
4. I. Reyero, G. Arzamendi and L. M. Gandía, *Chem. Eng. Res. Des.*, **92**, 1519 (2014).
5. V. G. Deshmane and Y. G. Adewuyi, *Fuel*, **107**, 474 (2013).
6. Y. M. Dai, J. S. Wu, C. C. Chen and K. T. Chen, *Chem. Eng. J.*, **280**, 370 (2015).
7. Y. M. Dai, K. T. Chen and C. C. Chen, *Chem. Eng. J.*, **250**, 267 (2014).
8. J. X. Wang, K. T. Chen, J. S. Wu, P. H. Wang, S. T. Huang and C. C. Chen, *Fuel Process. Technol.*, **104**, 167 (2012).
9. A. Buasri and V. Loryuenyong, *Green Process. Synth.*, **4**, 389 (2015).
10. Y. Y. Margaretha, H. S. Prastyo, A. Ayucitra and S. Ismadji, *Int. J. Energ. Environ. Eng.*, **3**, 33 (2012), DOI:10.1186/2251-6832-3-33.
11. D. Zeng, Q. Zhang, S. Chen, S. Liu, Y. Chen, Y. Tian and G. Wang, *J. Environ. Chem. Eng.*, **3**, 560 (2015).
12. A. Buasri, N. Chaiyut, V. Loryuenyong, P. Worawanitchaphong and S. Trongyong, *Sci. World J.*, **2013**, Article ID 460923, 7 pages (2013), DOI:10.1155/2013/460923.
13. Y. Tang, J. Xu, J. Zhang and Y. Lu, *J. Clean. Prod.*, **42**, 198 (2013).
14. Z. A. S. Nur, Y. H. Taufiq-Yap, M. F. R. Nizah, S. H. Teo, O. N. Syazwani and A. Islam, *Energy Convers. Manage.*, **78**, 738 (2014).
15. A. Buasri, K. Rochanakit, W. Wongvitvichot, U. Masa-ard and V. Loryuenyong, *Energy Procedia*, **79**, 562 (2015).
16. L. M. Correia, N. S. Campelo, D. S. Novaes, C. L. Cavalcante Jr., J. A. Cecilia, E. Rodríguez-Castellón and R. S. Vieira, *Chem. Eng. J.*, **269**, 35 (2015).
17. X. Liu, X. Piao, Y. Wang, S. Zhu and H. He, *Fuel*, **87**, 1076 (2008).
18. M. Kouzu, J. S. Hidaka, K. Wakabayashi and M. Tsunomori, *Appl. Catal. A*, **390**, 11 (2010).
19. M. López Granados, A. C. Alba-Rubio, F. Vila, D. Martín Alonso and R. Mariscal, *J. Catal.*, **276**, 229 (2010).
20. L. León-Reina, A. Aurelio Cabeza, J. Rius, P. Maireles-Torres, A. C. Alba-Rubio and M. López Granados, *J. Catal.*, **300**, 30 (2013).
21. S. H. Teo, U. Rashid and Y. H. Taufiq-Yap, *Energy Convers. Manage.*, **87**, 618 (2014).
22. S. Wahidin, A. Idris and S. R. M. Shaleh, *Energy Convers. Manage.*, **84**, 227 (2014).
23. Y. C. Lin, P. M. Yang, S. C. Chen and J. F. Lin, *Fuel Process. Technol.*, **115**, 57 (2013).
24. H. Masood, R. Yunus, T. S. Y. Choong, U. Rashid and Y H. T. Yap, *Appl. Catal. A*, **425-426**, 184 (2012).
25. A. Esipovich, S. Danov, A. Belousov and A. Rogozhin, *Fuel*, **107**, 474 (2014).
26. A. C. Alba-Rubio, F. Vila, D. M. Alonso, M. Ojeda, R. Mariscal and M. L. Granados, *Appl. Catal. B*, **95**, 279 (2010).
27. A. Buasri, T. Rattanapan, C. Boonrin, C. Wechayan and V Loryuenyong, *J. Chem.*, **2015**, Article ID 578625, 7 pages (2015), DOI: 10.1155/2015/578625.
28. M. Farooq, A. Ramli and D. Subbarao, *J. Clean. Prod.*, **59**, 131 (2013).
29. M. L. Granados, M. D. Z. Poves, D. M. Alonso, R. Mariscal, F. C. Galisteo, R. M. Tost, J. Santamaría and J. L. G. Fierro, *Appl. Catal. B*, **73**, 317 (2007).
30. P. Nair, B. Singh, S. N. Upadhyay and Y. C. Sharma, *J. Clean. Prod.*, **29-30**, 82 (2012).
31. Y. B. Cho and G. Seo, *Bioresour. Technol.*, **101**, 8515 (2010).
32. P. L. Boey, G. P. Maniam, S. A. Hamid and D. M. H. Ali, *Fuel*, **90**, 2353 (2011).
33. W. Suryaputra, I. Winata, N. Indraswati and S. Ismadji, *Renew. Energy*, **50**, 795 (2013).
34. M. Kouzu, T. Kasuno, M. Tajika, S. Yamanaka and J. Hidaka, *Appl. Catal. A*, **334**, 357 (2008).
35. S. H. Teo, A. Islam, T. Yusaf and Y. H. Taufiq-Yap, *Energy*, **78**, 63 (2014).
36. M. Hassan, Y. Robiah, S. Y. Thomas, U. Rashid and Y. H. Taufiq-Yap, *Appl. Catal. A*, **425-426**, 184 (2012).
37. B. Yoosuk, P. Udomsap and B. Puttasawat, *Appl. Catal. A*, **395**, 87 (2011).
38. A. R. Gupta, S. V. Yadav and V. K. Rathod, *Fuel*, **158**, 800 (2015).
39. S. Jaiyen, T. Naree and C. Ngamcharussrivichai, *Renew. Energy*, **74**, 433 (2015).
40. P. L. Boey, G. P. Maniam, S. A. Hamid and D. M. H. Ali, *J. Am. Oil Chem. Soc.*, **88**, 283 (2011).
41. O. Ilgen, *Fuel*, **92**, 452 (2011).
42. Y. C. Lin, S. C. Chen, C. E. Chen, P. M. Yang and S. R. Jhang, *Fuel*, **135**, 435 (2014).
43. P. Khemthong, C. Luadthong, W. Nualpaeng, P. Changsuwan, P. Tongprem, N. Viriya-empikul and K. Faungnawakij, *Catal. Today*, **190**, 112 (2012).
44. P. D. Patil, V. G. Gude, L. M. Camacho and S. Deng, *Energy Fuel*, **24**, 1298 (2010).
45. K. S. Chen, Y. C. Lin, K. H. Hsu and H. K. Wang, *Energy*, **38**, 151 (2012).
46. S. Singh and A. Patel, *J. Clean. Prod.*, **72**, 46 (2014).

47. D. D. Bala, K. Souza, M. Misra and D. Chidambaram, *J. Clean. Prod.*, **104**, 273 (2015).
48. A. Buasri, N. Chaiyut, V. Loryuenyong, C. Rodklum, T. Chaikwan, N. Kumphan, K. Jadee, P. Klinklom and W. Wittayarounayut, *Sci. Asia*, **38**, 283 (2012).
49. A. Obadiah, G. A. Swaroopa, S. V. Kumar, K. R. Jeganathan and A. Ramasubbu, *Bioresour. Technol.*, **116**, 512 (2012).
50. M. Farooq, A. Ramli and A. Naeem, *Renew. Energy*, **76**, 362 (2015).
51. G. Joshi, D. S. Rawat, B. Y. Lamba, K. K. Bisht, P. Kumar, N. Kumar and S. Kumar, *Energy Convers. Manage.*, **96**, 258 (2015).
52. A. Buasri, B. Ksapabutr, M. Panapoy and N. Chaiyut, *Korean J. Chem. Eng.*, **29**, 1708 (2012).

## APPENDIX A

Energy Efficiency Calculation:

$$\text{Energy efficiency (g/J)} = \frac{\text{Amount of biodiesel formed (g/L)}}{\text{Energy consumed (J/L)}}$$

Power of microwave=600 W; Reaction time=3 min=180 s; Consumed energy of biodiesel production=$1.08\times10^5$ J

Reaction volume=0.050 L

Heating value of *Jatropha* biodiesel=42.15 MJ/kg

Energy dissipated per unit volume=$1.08\times10^5/0.05=2.16\times10^6$ J/L

Amount of biodiesel formed by using $Ca(OCH_3)_2$ catalyst=872.46 g/L

Energy efficiency of biodiesel production by using $Ca(OCH_3)_2$ catalyst=$872.46/2.16\times10^6=4.03\times10^{-4}$ g/J=16.98 MJ/MJ

Amount of biodiesel formed by using $Ca[O(OH)_2C_3H_5]_2$ catalyst=873.91 g/L

Energy efficiency of biodiesel production by using $Ca[O(OH)_2C_3H_5]_2$ catalyst=$873.91/2.16\times10^6=4.05\times10^{-4}$ g/J=17.07 MJ/MJ

Amount of biodiesel formed by using CaO catalyst=794.70 g/L

Energy efficiency of biodiesel production by using CaO catalyst=$794.70/2.16\times10^6=3.68\times10^{-4}$ g/J=15.51 MJ/MJ

Energy Efficiency of Catalyst for Biodiesel Production:

$Ca[O(OH)_2C_3H_5]_2>Ca(OCH_3)_2>CaO$

Power of furnace=1,800 W; Calcination time=2 h=7,200 s; Consumed energy of calcination=$1.296\times10^7$ J

Power of hotplate and magnetic stirrer=500 W; Reaction time=8 h=28,800 s; Consumed energy of catalyst modification=$1.44\times10^7$ J

Energy dissipated per unit volume by using $Ca(OCH_3)_2$ and $Ca[O(OH)_2C_3H_5]_2$ catalysts=$(1.08\times10^5+1.296\times10^7+1.44\times10^7)/0.05=5.49\times10^8$ J/L

Energy efficiency of overall process by using $Ca(OCH_3)_2$ catalyst=$872.46/5.49\times10^8=1.59\times10^{-6}$ g/J

Energy efficiency of overall process by using $Ca[O(OH)_2C_3H_5]_2$ catalyst=$873.91/5.49\times10^8=1.59\times10^{-6}$ g/J

Energy dissipated per unit volume by using CaO catalyst=$(1.08\times10^5+1.296\times10^7)/0.05=2.61\times10^8$ J/L

Energy efficiency of overall process by using CaO catalyst=$794.70/2.61\times10^8=3.04\times10^{-6}$ g/J

Energy Efficiency of Catalyst for Overall Process:

$CaO>Ca(OCH_3)_2=Ca[O(OH)_2C_3H_5]_2$